Hindawi
Advances in Civil Engineering
Volume 2022, Article ID 6845847, 12 pages
https://doi.org/10.1155/2022/6845847

Research Article

Study on Distribution Characteristics of Metro Stray Current and Evaluation of Cumulative Corrosion Effect

Shan Lin,[1] **Jing Zhang**,[2] **Xuehua Liu**,[2] **Xianwei Zhang**,[2] **Zhichao Cai**,[2] **and Xia Chen**[1]

[1]*Guangzhou Metro Design & Research Institute Co., Ltd., Guangzhou 510010, China*
[2]*School of Electrical and Automation Engineering, East China Jiaotong University, Nanchang 330013, China*

Correspondence should be addressed to Zhichao Cai; czchebut@foxmail.com

Received 14 October 2021; Accepted 13 December 2021; Published 10 January 2022

Academic Editor: Yuan Mei

Stray current directly affects the regular operation of electrical equipment and facilities in the subway DC traction power supply system. Therefore, it is worthwhile to study the stray current distribution characteristics during train operation and the quantitative corrosion of buried pipelines. This paper introduces the traction characteristics of power carriages and power wheelsets of subway vehicles into the DC traction process. A finite element model considering the dynamic distribution of stray current under the actual operation of subway vehicles is established. The interference characteristics of stray current and the contribution of power sources under the multiparticle model are analyzed. The rail insulation damage caused by long service time and the quantitative calculation of rail and buried pipeline corrosion is considered. The model results show that the stray current in the buried pipeline under the multiparticle model is more accurate and more suitable for the protection in the actual subway. The quantitative corrosion of the buried pipeline is stronger than the partial insulation damage environment when the rail is not insulated. The rail and buried pipeline corrosion at both ends of the insulation damage position is relatively severe. The stray current distribution model established in this paper gives full play to the solution advantages of the finite element method and provides a new idea for the quantitative calculation of buried pipeline corrosion.

1. Introduction

With the development of China's national economy and the promotion of urbanization, urban rail transit has been vigorously developed as an effective tool to alleviate traffic congestion. DC electric traction is adopted in urban rail transit systems such as subway and light rail. The train receives power through the pantograph or collector boots, and the rail is used to achieve reflux. In the initial stage of subway operation, the degree of insulation between the steel rail and the underground metal structure is relatively high, the rail-to-ground transition resistance is rather large, and the stray current leaking from the steel rail to the surrounding soil medium is also relatively small. However, with the increase of the working life of the subway, the rail-to-ground insulation performance of the rail decreases, and the stray current leaking from the rail to the surrounding soil medium will increase [1]. Therefore, the metro equipment that has been built and used for a long time is easy to lead to the corrosion of underground metal structures under the interference of rail overpotential and stray current [2–4].

According to the existing subway traction power supply system, domestic and foreign scholars have alleviated the leakage of rail overpotential and stray current by controlling rail return mode [5–7], blocking current leakage [8–15], and protecting affected structural parts [16–23]. For example, increasing the supply voltage is helpful to reduce the rail current [5]. The use of minimizing the distance between DC railway substations helps to shorten the leakage path of track current [5]. A fully insulated rail is installed as a special return rail to transfer the return current from the rail to the special return rail [6, 7]. Concrete sleepers, side column insulators, insulating clips, and rail cushions are used to insulate the track from the ground, blocking or reducing the leakage path of track current [8–10].

Therefore, this paper establishes the finite element distribution model of stray current to analyze the interference quantitatively. The operating parameters of actual subway vehicles are selected to be easy to measure and a dynamic stray current interference calculation example is proposed. The main contributions are as follows:

(1) Considering the current distribution and marshaling configuration inside the train, combined with the actual running state of the subway vehicle, the stray current leakage is analyzed when the bullet train carriage is used as the particle and the train wheel as the particle backflow. Furthermore, the contribution of the leakage degree of each power car provides reference information for additional protection measures such as cathodic protection.

(2) As part of the rail insulation is damaged in the section of the subway with long operating life, the influence of rail insulation damage on the distribution of stray current is analyzed, and the total current density and corrosion area of rail corrosion in the section are analyzed when the location of insulation damage and the size of the damaged area is different.

(3) According to the distribution of rail potential and current density of buried pipeline, the cathode area and anode area of the buried pipeline at any time are determined, and the relationship between current leakage position and buried pipeline corrosion under different conditions is analyzed.

The content of this paper is arranged as follows: Section 2 shows the theoretical analysis modeling process and solution process of corrosion current on the buried pipeline; Section 3 discusses the distribution characteristics of rail potential and stray current under the condition of multiparticle distribution; Section 4 gives the dynamic cathode and anode area changes of stray current, the corrosion accumulation of metal structures, and the insulation damage of some areas causing new stray current interference. Finally, Section 5 gives the conclusion.

2. Model Establishment and Solution

In urban rail transit, the typical configuration of the subway traction power supply system is shown in Figure 1. The power grid powers the subway system, and the main substation is reduced from AC110 kV to AC35 kV by the transformer. Then it is divided into two parts. One part is reduced by the rectifier transformer in the traction substation to AC 1180 v voltage and converted into DC1500V or (DC750V) through a 24 pulse rectifier circuit to supply power to the catenary. After the contact between the pantograph and catenary, it provides traction current to the train and drives the train to run. The other part is reduced to AC voltage of 380 V through the transformer of the station substation, which supplies power to the elevator, ventilation system, lighting, and other electrical equipment in the station.

This paper draws the traction current and running speed curve of the train based on the operational data of the Nanchang Metro Line 1 Metro Central Station to the Qiushui Square Station, as shown in Figure 2. The train has different traction currents at any time so that it can be regarded as a movable current source and the whole loop system as a constant electric field in the model.

2.1. Modeling. According to the analysis of the subway mentioned above power supply system, a finite element solution model including locomotives, stations, tracks, soil, and buried pipelines is established, as shown in Figure 3. The model mainly includes four parts: the construction of geometry, the addition of physical field, meshing, and post-processing. The geometric size of the soil domain is $1500 \times 150 \times 100$ m, the wheel radius is 0.5 m, and the setting size of steel rail is $1500 \times 0.5 \times 0.1$ m. The buried pipeline is located 30 m directly below the rail, with a length of 1500 m and a radius of 1 m. According to the above dimensions, a finite element model is established in COMSOL Multiphysics. Since the train has traction current at any time, the current module is added to treat the train as a current source, and the inner wheel of the train is the input boundary of the traction current as of the terminal of the model. The two ends of the subway section are set as the negative poles of the substation, which are directly grounded to study the distribution of stray current in the soil under the mobile current source and its corrosion effect on buried pipelines. The finite element method divides a continuous solution region into a set of element combinations. It uses the approximate functions of these elements to express the unknown positions of the solution domain. Therefore, the accuracy of the model solution depends on the precision of meshing. According to the computational accuracy and efficiency requirements, the solution domain of the model is divided into 30637 domain elements and 2068 boundary elements through free triangular meshes.

Since this paper considers the distribution of actual subway vehicles, in the process of establishing the model, if other parameters are the same, the multiparticle model 1 is based on the number of power cars in the subway train formation, and the multiparticle model 2 is based on the number of moving wheelsets of the train. The differences of each model are shown in Table 1.

The traction current flows into the wheel from the positive pole of the traction substation through the catenary, pantograph, high-speed circuit breaker, traction inverter, coupling, and gearbox. The wheel current distribution is shown in Figure 4. Since the traction current in Figures 4(a) and 4(b) has the same current size and different directions at the time of acceleration and deceleration, the current path in reflux is very different. At the time of train acceleration (when the current is positive), the traction current is transferred from the connection between the wheel and the axle to the tread where the axle is in contact with the rail. Most of the current is transmitted from both sides of the tread contact surface to the traction substations on the left and right sides through the rail, but very little of the current

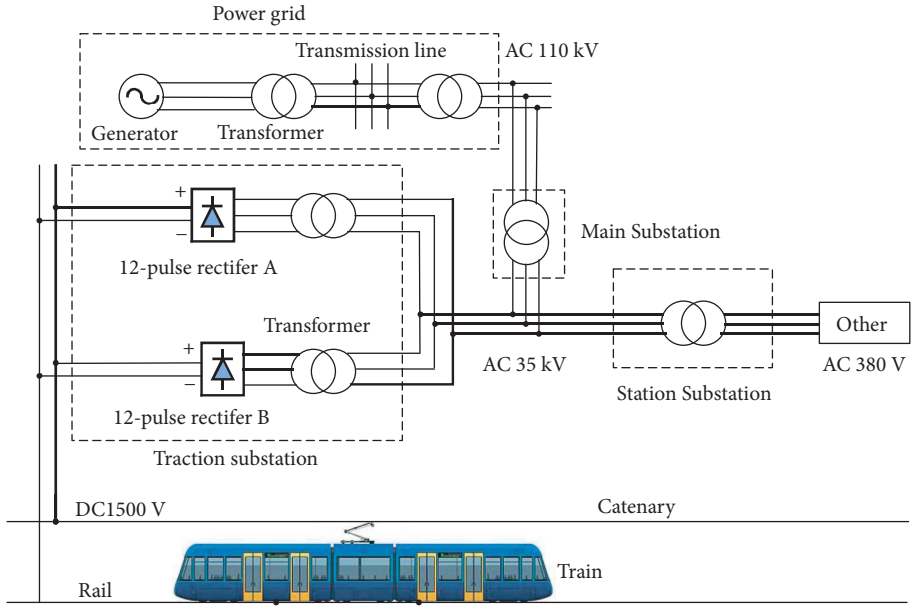

Figure 1: Schematic diagram of subway traction power supply system.

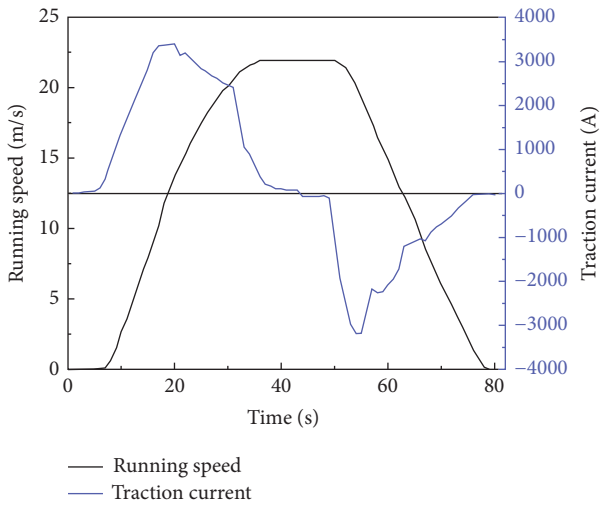

Figure 2: Train running speed and traction current.

leaks from the rail to the soil. At the time of train deceleration (due to the influence of current receiving power, the current is negative at this time), according to the principle of regenerative braking, most of the current is fed back to the positive pole of traction substation through catenary current, to reduce energy loss. However, very little of the current leaks into the soil from the rails, thus corroding the rails and buried pipelines.

Considering that the stray current distribution is a constant electric field problem, some simplifications and assumptions are made that the soil near the pipeline is uniformly distributed and the concentration gradient in the soil is ignored. The finite element method is used to solve the Maxwell equation, and the "AC/DC module" can solve the Maxwell equation.

Governing equation is

$$\begin{aligned} \nabla \times E &= 0, \\ \nabla \cdot J &= 0. \end{aligned} \tag{1}$$

The current density J in soil electrolyte obeys Ohm's law, and its constitutive relation is as follows:

$$J = \gamma E. \tag{2}$$

The interface conditions in the model meet

$$\begin{aligned} E_{1t} &= E_{2t}, \\ J_{1n} &= J_{2n}, \end{aligned} \tag{3}$$

where E represents the electric field strength, J represents the current area density, γ represents conductivity, E_t represents the tangential component of electric field strength, and J_n represents the normal component of current area density.

The soil and buried pipeline are set as constant conductivity, 1 E − 2 S/m and 1 E7 S/m, respectively. For simplicity, the conductivity of metals (such as rails, train wheels) is also set to 1 E7 S/m [24].

2.2. Solution of Corrosion Current Density of Metal Structures under Stray Current Interference. Due to the dynamic changes of underground metal potential during the subway operation period, the metal surface is easy to reach the primary conditions of electrochemical corrosion. Then the buried metal pipelines around the subway and the steel bars in the main structure of the station and section tunnels will be electrochemically corroded. Electrochemical corrosion will shorten the service life of metal pipelines and reduce the strength and durability of the subway's reinforced concrete [25–30].

When the dynamic stray current flows into the pipeline, the pipe section is called the cathode area and will not be corroded. However, cathodic polarization can increase soil

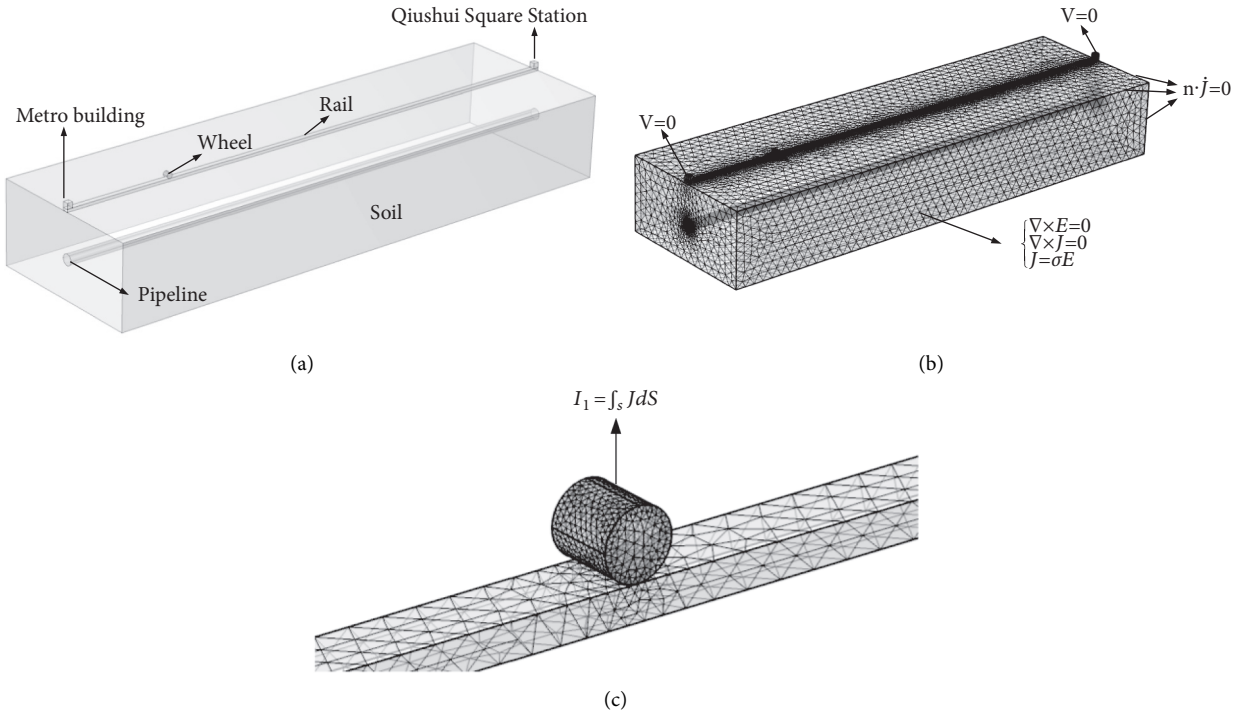

Figure 3: Finite element solution model. (a) Solid geometry diagram. (b) Overall meshing. (c) Local meshing.

Table 1: Modeling methods of different models.

Models	Modeling method
Single particle model	Regard the train as a whole as a particle.
Multiparticle model 1	According to the four-motion and two-drag grouping mode, each power car is regarded as a particle.
Multiparticle model 2	According to the fact that there are two switch machines in each power car to control four moving wheelsets, each wheelset is regarded as a particle.

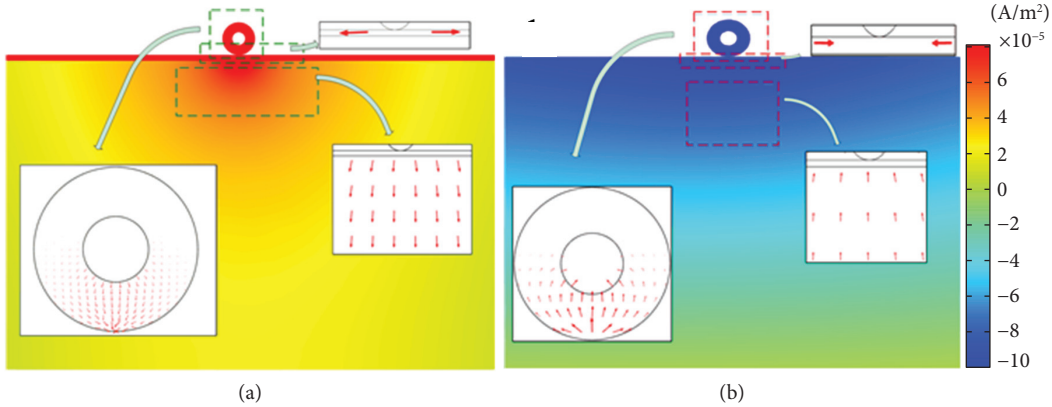

Figure 4: Traction current reflux path. (a) Positive traction current. (b) Negative traction current.

pH value (alkaline) around the damage point of the pipeline anticorrosion layer, which will reduce the adhesion of the anticorrosion layer and the peeling off of the anticorrosion layer. When the density of the DC stray current flowing into the pipeline is too high, it will cause the hydrogen evolution reaction, which may cause hydrogen embrittlement of high-strength pipes. In the area where the stray current flows out (anode area), electrons flow from the anode to the cathode,

while ions flow in the surrounding soil. The oxidation process leads to the dissolution or loss of metal. Therefore, stray current directly leads to the corrosion of steel bars and reduces the reinforced concrete. The service life of the structure is reduced. Since the stray current changes dynamically, there will be alternating changes of the cathode area and the anode area at the same position on the pipeline. It can be seen from Figure 5 that there are mainly two places where the traction current leaks: area A directly below the train during the operation of the subway vehicle and area D directly below the traction substation. At the same time, it is verified that both leakage current and stray current are dynamic changes, and the corrosion of rail and pipeline is interlaced. When electrochemical corrosion occurs at rail A, no corrosion occurs directly below the rail at the corresponding buried pipeline B.

The finite element model can calculate the leakage current density $i(t)$ of the buried pipeline. If the current density in the anode region is $i_1(t)$ and that in the cathode area is $i_2(t)$, the leakage current density of the buried pipeline can be satisfied.

$$i(t) = i_1(t) + i_2(t). \tag{4}$$

Since the current density in the cathode area will not corrode the buried pipeline, considering only the anode corrosion current density $i_1(t)$, the corrosion current density of the pipeline at each moment is $i_f(t)$:

$$i_f(t) = i_1(t). \tag{5}$$

The total current area density of (T) of the cumulative corrosion of the whole pipeline is

$$i_F(t) = \sum_{t=1}^{T} i_f(t) = \sum_{t=1}^{T} i_1(t), \tag{6}$$

where $T = 1s, 2s, \ldots, 83s$, T is the total operation time of the train in a single operation section.

Since all leakage currents are dynamic and the corrosion current density leaked from each rail and buried pipe is a function of time [9], we can define the time integral of the leakage corrosion current density $i_f(t)$ as the total leakage charge Q:

$$Q = \int_{t_1}^{t_2} i_f(t)\mathrm{d}t. \tag{7}$$

According to Faraday's law, the weight of rail corrosion metal is proportional to the total leakage charge [31], so the corrosion current density can be used as an objective parameter to evaluate rail corrosion indirectly.

3. Consider the Effect of Multiple Current Sources on Stray Current

Traditional stray current analysis models generally use a single-particle model (using a vehicle as a current source of particles), common in analytical solutions. Cai et al. [32] studied the influence of the subway track on the stray current of the ground transition resistance under the single-mass model. Xu [33] established a continuous track-drainage network-earth-buried pipeline based on the single-mass model and calculated the pipeline and earth resistance. Yang et al. [34] established a mathematical model of the rail potential distribution of the entire line based on the single-particle model, revealing the subway rail potential distribution law considering the edge effect of the finite boundary. However, simplifying the single-particle model for the train will affect the actual stray current distribution, so introducing a multiparticle model is considered. In a more optimized situation, a power car can be used as a particle current source (multiparticle model 1, considering the relative distance between the power cars) and a set of moving wheels as a particle current source (multiparticle model 2, viewing the close distance between the moving wheels), as shown in Figure 6. By comparing the three models, it is found that the rail potential and the trend distribution of stray current obtained by the calculation are consistent. However, the result of the single-particle solution is slightly larger than that of the multiparticle model, which may happen although the length between the motor cars is shorter than that of an interval, and it cannot be ignored that there still be an impact on the steel pipe potential and stray current. The same problem exists when considering the multiwheel situation. Because the multiparticle model is closer to the actual operation, the result is more relative to the existing subway system, making pipeline corrosion calculation and analysis more accurate.

According to the train formation of the subway vehicles of Nanchang Metro Line 1, the four power cars in the vehicles are concentrated in the central area. The relative distance maintains a car's length. Stray current leakage occurs in each power car, and the leakage position is consistent with the relative position of each carriage. The current is leaked to both sides. The buried pipeline produces the maximum stray current at the relative position between the carriage and the traction substation, as shown in Figure 6. Although the traction current gap in each carriage is minimal, the influence of each power car on the stray current of the whole buried pipeline is significantly different, as shown in Figure 7. Since the multiparticle model 1 analyzes the train carriage as a particle, the four particles from left to right are called power car 1, power car 2, power car 3, and power car 4, respectively. The train runs from left to right. In the initial stage of subway vehicle operation (traction state), the first power car (power car 4) in the forward direction of the subway vehicle has the most significant contribution and drives the train. In the stage of constant speed operation of subway vehicles, the contribution of each power car is the same to keep the train running at a constant speed. In the stop phase (braking phase) of subway vehicles, the fourth power car (power car 1) in the forward direction contributes the most. It is worth noting that the division of the areas mentioned above does not entirely correspond to the operating conditions of subway vehicles. However, the more stray current is indeed leaked from the power cars at both ends of the subway vehicles. In contrast, the stray currents leaked from other power cars are relatively minor. In the operation section, the power car closest to the middle

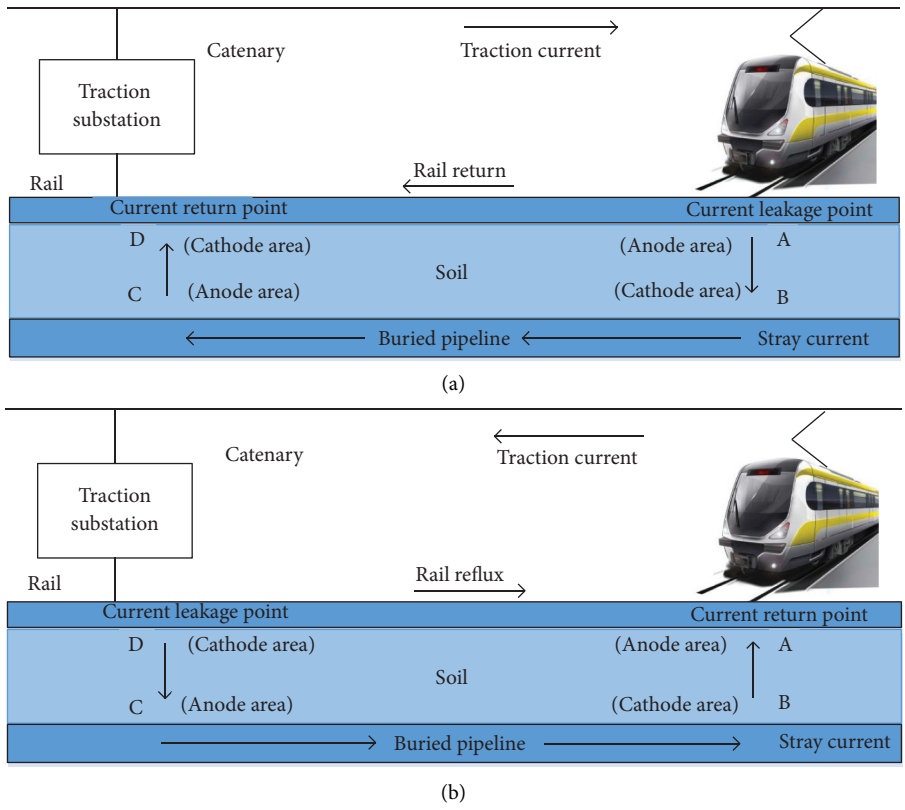

Figure 5: Electrochemical corrosion caused by stray current. (a) Train traction current is positive. (b) Train traction current is negative.

position will return more traction current to the traction substations on both sides through the rails. In contrast, other power cars will return most of the traction current to the traction substations on both sides through the rails. Therefore, a small part of the current leaked into the soil, causing the buried pipeline to be destroyed.

4. Effect of Rail Insulation Damage on Stray Current Distribution

4.1. Quantitative Analysis of Rail Corrosion under Stray Current Interference. Rail corrosion refers to the electrochemical corrosion of the rail at the leakage current, which leads to severe corrosion at the bottom of the rail, and the existing fasteners are not enough to make the corroded rail safely fixed on the sleeper. It is also noteworthy that there are dynamic changes in the position of rail corrosion; that is, where the subway vehicle runs, the relative position of its contact with the rail bottom will produce oxidation reaction and electrochemical corrosion. Theoretically, the wheel is in point-line contact with the rail, and the corresponding corrosion is also point-line corrosion. The oxidation reaction is mainly the loss of electrons, and the more significant the oxidation reaction rate, the greater the number of losses of electrons. Therefore, the more the traction current leaks, the more pronounced the electrochemical corrosion. The specific redox reaction equation is as follows:

$$\begin{aligned}
\text{anode: } & 2Fe - 4e^- = 2Fe^{2+}, \\
\text{cathode: } & 4H^+ + 4e^- = 2H_2\uparrow \text{(anaerobic acidic environment)} \\
& 4H_2O + 4e^- = 4OH^- + 2H_2\uparrow \text{(anaerobic environment)} \\
& O_2 + 2H_2O + 4e^- = 4OH^- \text{ (aerobic alkaline environment)}
\end{aligned} \tag{8}$$

The analysis shows that the area of rail leakage current is related to the running state of the train without the insulation between rail and soil. When the train is in the acceleration state, the rail leakage current area is consistent with the contact area of the rail wheelset; when the train is in the deceleration state, the rail leakage current area is consistent with the substation area. When the isolation condition between rail and soil is applied, if damage occurs in a certain area, no matter where the subway vehicle is running, the breakage area or traction substation area will produce current leakage. Therefore, the electrochemical corrosion in the breakage area and the area near the substation will be more serious, as shown in Figure 8. Because the traction current flows in different directions at different times, the potential in the soil changes continuously. When the traction current is in the opposite direction, the potential change in the soil is also just the opposite. The protection of the insulating layer can better guide the loop current on the steel rail and collect it to the negative pole of the traction substation. The difference is that under the condition of no

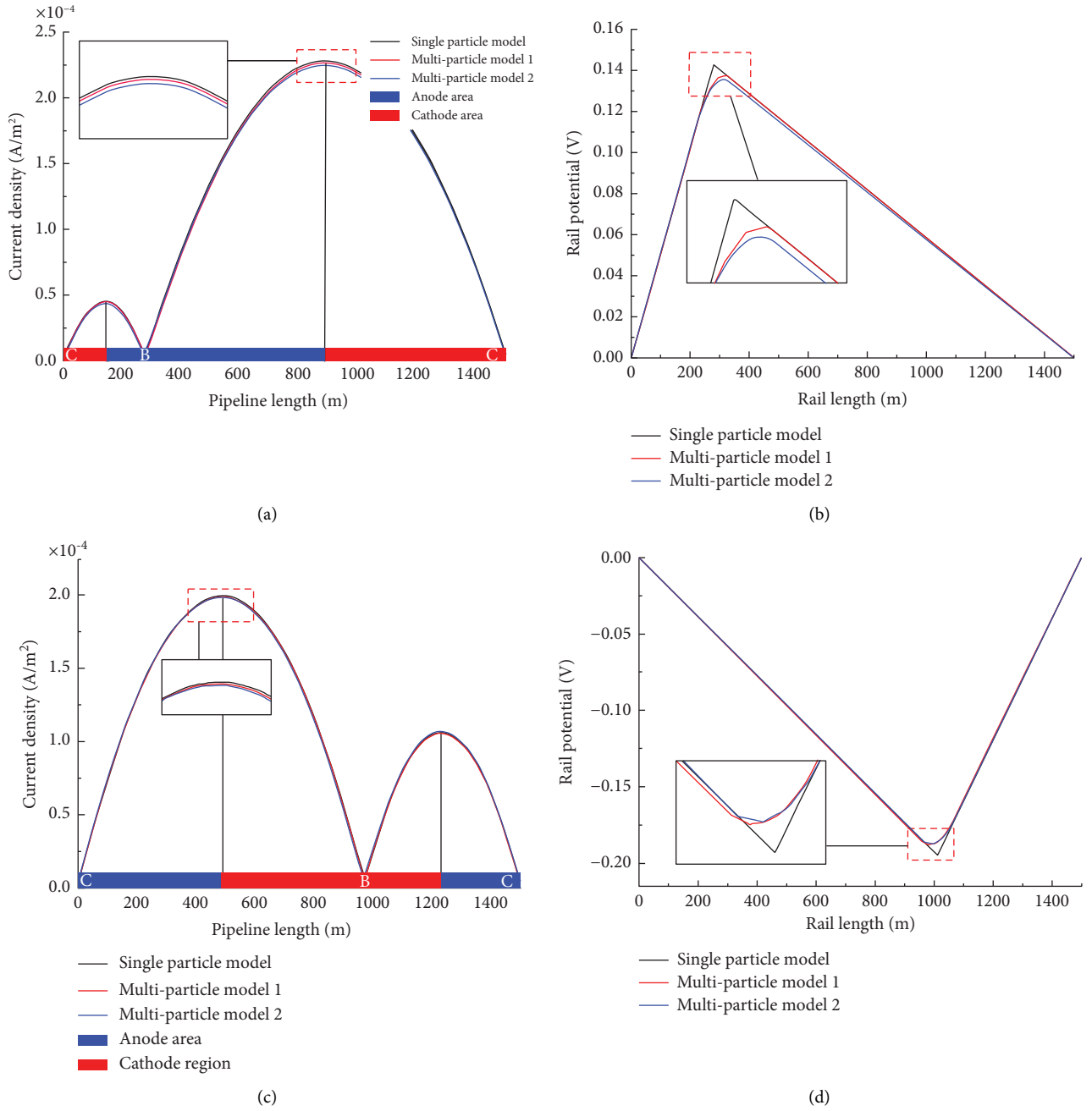

Figure 6: Analysis of the influence of each model on stray current and rail voltage. (a) Pipeline current density ($t = 20$ s). (b) Rail potential ($t = 20$ s). (c) Pipeline current density ($t = 55$ s). (d) Rail potential ($t = 55$ s).

insulation, the leakage area covers the whole rail, while under the condition of insulation, leakage always occurs in the insulation damage area, which accelerates the redox reaction there.

Figure 9 is a comparison diagram of rail corrosion current when the rail is without insulation and when the rail is insulated, but the insulation is damaged at different positions. At this time, the length of the rail damage is the same, and the position is different, as shown in Table 2. When the insulation is added to the rail, the leakage of current in the rail interval can be reduced obviously. When some physical or human factors damage the insulation layer at a specific position, it can be seen that the rail has apparent current leakage at the damaged position. The leakage current makes the oxidation rate of the rail more significant. It accelerates the corrosion of the damaged part of the rail, thereby leading to some hidden safety problems. The rail corrosion current is in a "concave" shape at both ends of the damaged insulation. Compared with the middle of the damaged position, there is more corrosion current leakage at both ends of the damaged insulation. This shows that at the junction of damaged and undamaged insulation, the corrosion current is the largest, leading to the most severe corrosion of the steel rail. Still, it reduces the corrosion of the rail near the traction substation

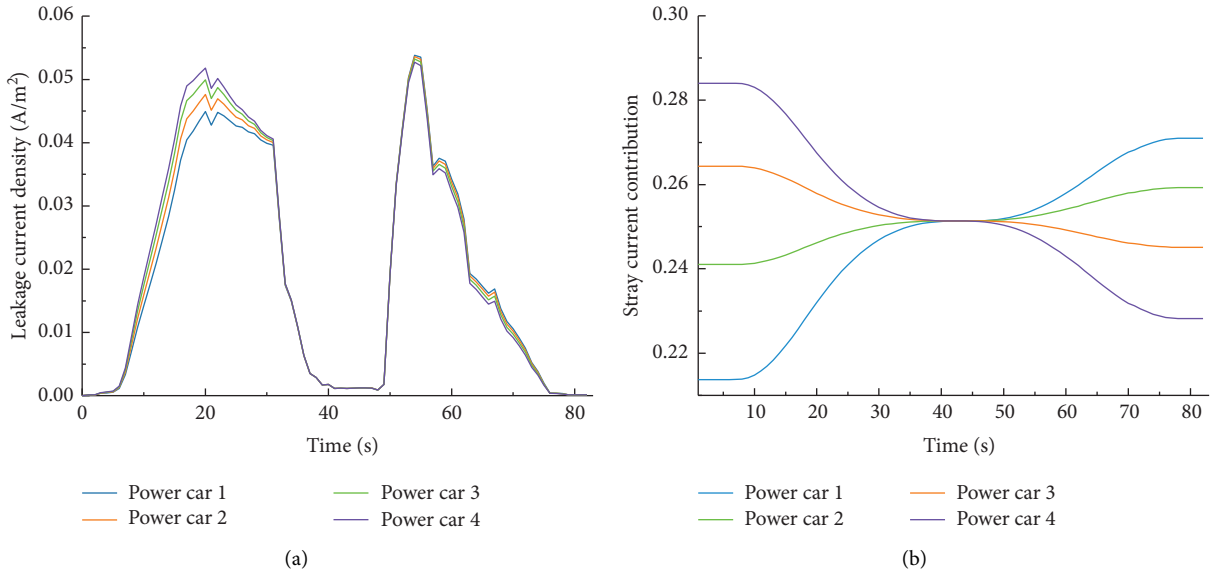

Figure 7: Analysis of the influence of each power car on stray current in the multiparticle model 1. (a) Leakage of each power car. (b) Contribution of power car.

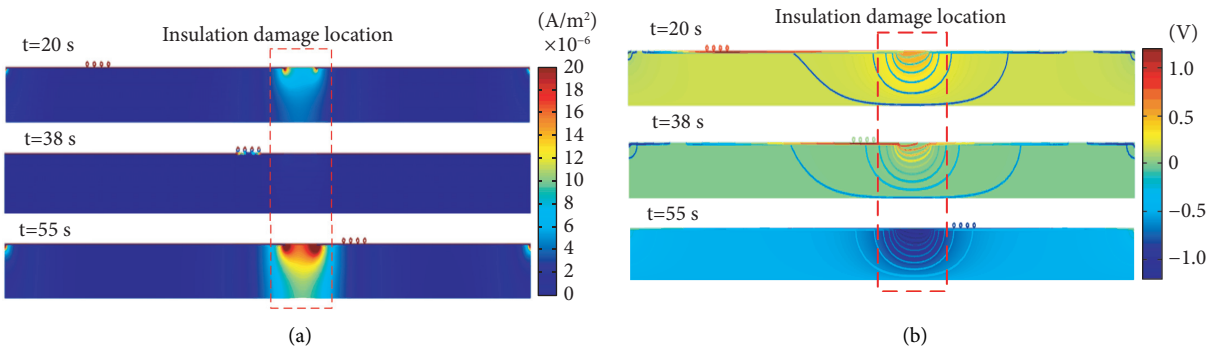

Figure 8: Distribution in soil at different times (when partial insulation is broken). (a) Current leakage. (b) Potential distribution.

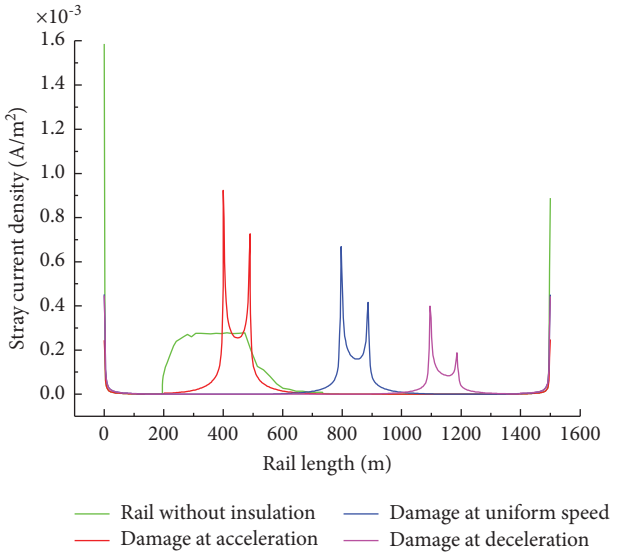

Figure 9: Total corrosion current density of rail under different conditions.

when the rail is not insulated. In the middle of insulation damage, the rail corrosion current is relatively small. When the train runs at both ends, the rail returns current first passes through the junction of insulation damage and sound insulation, resulting in most current leakage at the junction point. In contrast, the damage in the middle is relatively more minor. Affected by the distance and traction current, the current density of damaged rail corrosion is the acceleration, constant, and deceleration time in descending order. The corrosion current density of the rail near the traction substation is just the opposite of the corrosion current density of the damaged place.

If there is a damaged area of rail insulation, with the train running in this section, the damaged area's size is different, leading to the severity of rail corrosion. If the damaged area is tiny and approaches a point, all the stray current leaks at that point, resulting in severe damage to the rail. When the damaged area gradually becomes more extensive, the corrosion current of the rail will be slowed down, but the corrosion area of the rail will increase. As shown in

Table 2: Location and length parameters of rail insulation damage.

Type	Insulation damage location (m)	Insulation damage length (m)
Damaged acceleration	400–490	90
Damaged at constant speed	800–890	90
Damaged at deceleration	1100–1190	90
45 m damaged at acceleration	422.5–467.5	45
180 m damaged at acceleration	355–535	180

Figure 10, taking insulation damage of 45 m, 90 m, and 180 m as examples, as the damage area increases by multiples, the rail corrosion current gradually decreases. When the rail insulation is completely damaged, the corrosion current in the rail section reaches the minimum, but it changes. The corrosion current near the power station reaches its maximum.

4.2. Quantitative Analysis of Buried Pipeline Corrosion under Stray Current Interference. Pipeline corrosion refers to the corrosion problem caused by the stray current in the anode area of buried pipelines. Since the magnitude and direction of the stray current are constantly changing, it will cause dynamic DC stray current interference to the pipeline. At the same time, there are dynamic changes in the location and degree of corrosion of buried pipelines. Therefore, dynamic pipeline corrosion needs to be quantitatively analyzed.

Firstly, the buried pipeline is divided into cathode and anode regions. From the previous distribution of the stray current on the surface of the pipeline at a specific time, it can be seen that there are two peaks of the stray current on the surface of the steel pipe, corresponding to the critical value of the current inflow and outflow of the buried pipeline. When the current flows forward, the rail position corresponding to the inner side of the two wave crests is the cathode area, and the rail position corresponding to the outer side of the two wave crests is the anode area. Conversely, when the current flows in the reverse direction, the rail position corresponding to the inner side of the two wave peaks is the anode area, and the rail position corresponding to the outer side of the two wave peaks is the cathode area, as shown in Figures 6(a) and 6(c). Position B in Figure 6 is the position where the train is located, and position C is the position corresponding to the traction substation, which corresponds to the position in Figure 5.

By comparing noninsulated conditions and insulation damage, the size of the pipeline's cathode area and anode area is the same under noninsulated conditions. In the case of insulation damage, the cathode and anode areas of the pipeline have apparent size changes. When the traction current flows positively, the anode area is larger than the cathode area. On the contrary, the anode area is smaller than the cathode area. It can be concluded that when the traction current is positive, the anode area is inversely proportional to the width of insulation damage, and when the traction current is negative, the anode region is proportional to the width of insulation damage.

According to the division of the cathode and anode areas of the buried pipeline, the leakage current density of the

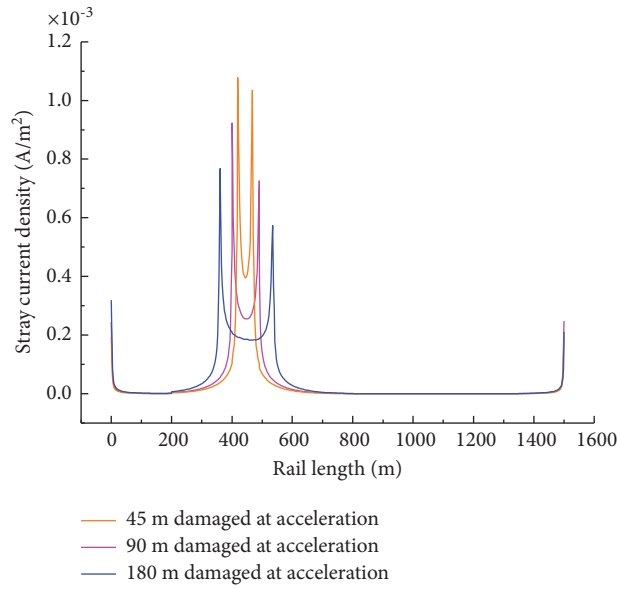

Figure 10: Corrosion current density of rail with different damage length.

anode area is accumulated. The total corrosion current density of the buried pipeline in the section is calculated, forming a dynamic cumulative electrochemical corrosion effect of stray current on the buried pipeline. The calculation flow chart is shown in Figure 11.

Since the calculation of the model can directly obtain the leakage current density in the buried pipeline, the leakage current density of the damaged pipeline at the acceleration is shown in Figure 12(a). According to the calculation process of the flowchart, the corrosion area of the buried pipeline and the corresponding corrosion current density can be obtained at each moment, and the corrosion current density of the buried pipeline damaged at the acceleration is shown in Figure 12(b). By superimposing the corrosion current density of the same area at each time, the corrosion area and the corresponding corrosion current density of the entire buried pipeline in the section can be obtained.

The calculation flow chart of the corrosion current density of the buried pipelines is shown in Figure 13. The corrosion situation of the stray current at the specific location of the pipeline can be obtained, which is convenient for the reasonable evaluation of the quantitative corrosion caused by the subsequent stray current. When there is no insulation, the cathode and anode areas of the pipeline are theoretically the same. The cumulative analysis of the dynamic pipeline corrosion current density shows that there is still a large oxidation reaction interference area, which is

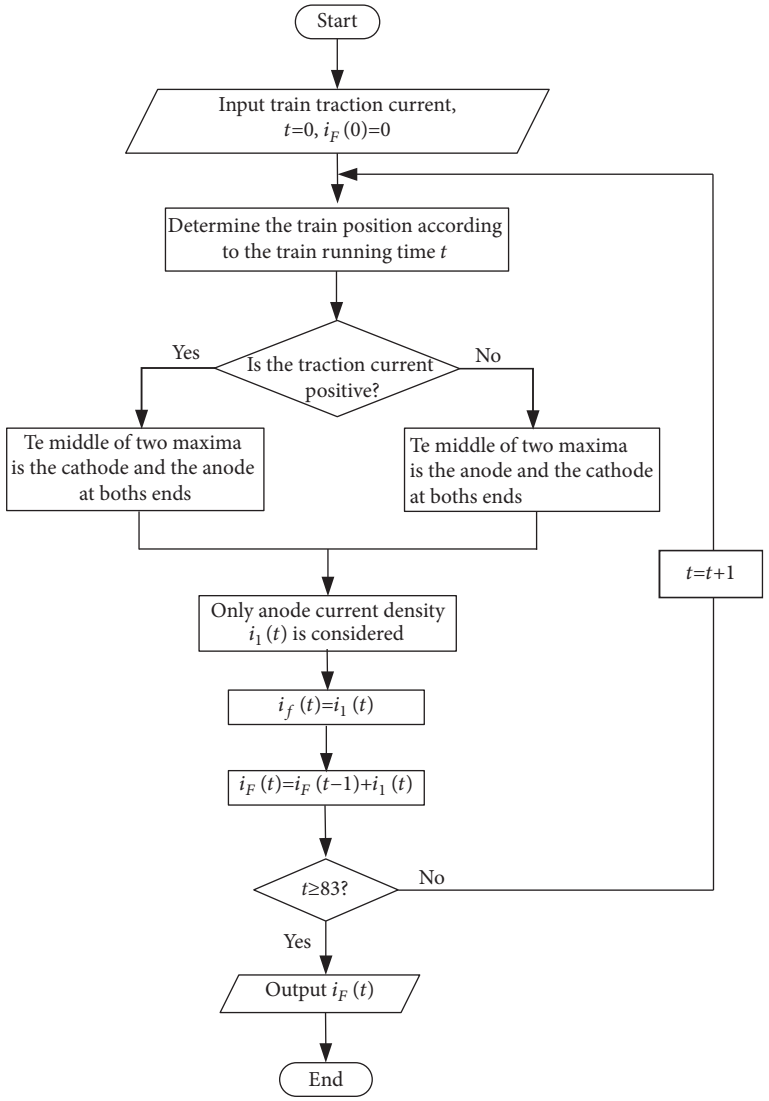

Figure 11: Flowchart for calculation of total corrosion current density of buried pipelines.

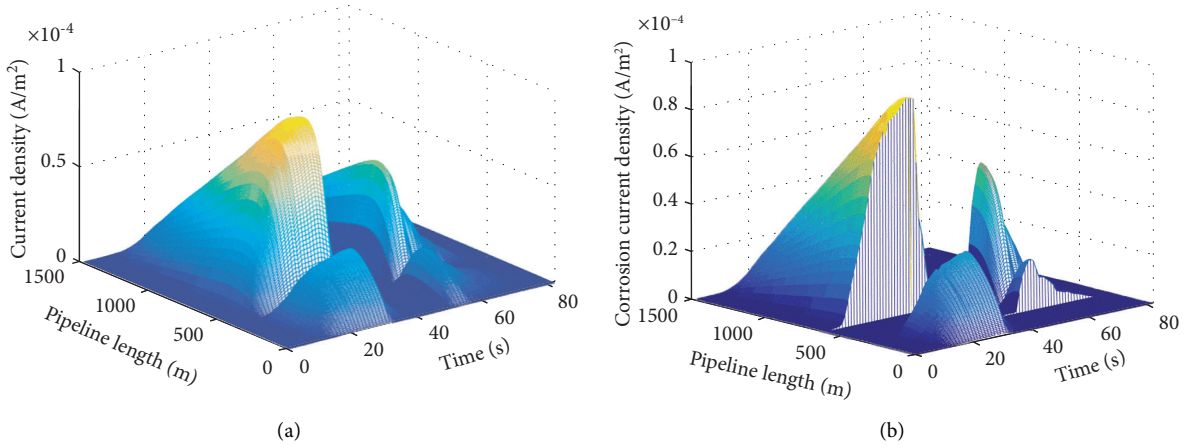

Figure 12: Distribution of current density on the pipeline in the section. (a) Leakage current density of pipeline damaged at acceleration. (b) Corrosion current density of pipeline damaged at acceleration.

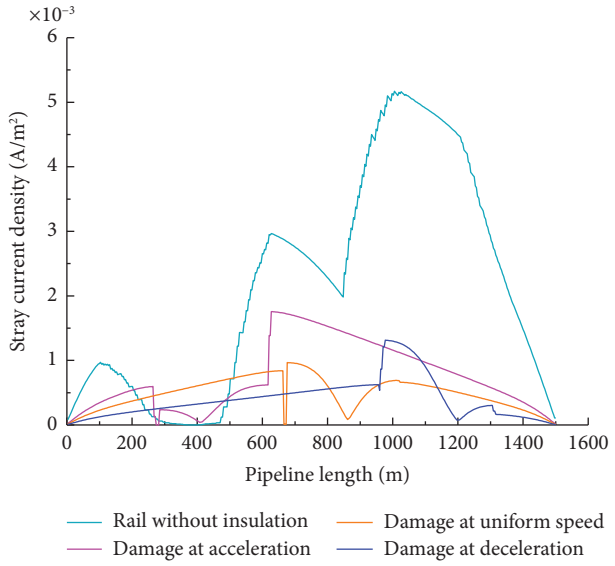

Figure 13: Corrosion of buried pipelines in train operation section.

significantly more potent than the insulation. The dynamic corrosion accumulation caused by insulation damage is relatively fixed; both ends show an increasing trend towards the damaged area. There are rapid increases and decreases around the damaged position. Compared with the insulation damage that occurred in different areas, corrosion accumulation is different, and the cumulative corrosion in the deceleration area is slight.

5. Conclusions

The distribution of stray current is affected by multiparameter variables. This paper considers the distribution and operation of actual subway vehicles and the electrochemical corrosion caused by the failure of relevant mitigation measures to use the stray current finite element model to guide the engineering practice and ensure subway vehicles' safe and stable operation. The main conclusions are as follows:

(1) The multiparticle model is more consistent with the actual running state of subway vehicles than the single-particle model. After solving and comparing, the stray current calculated by the multiparticle model is relatively small and has low pipeline potential. At the same time, the front wheel leakage of the train during the starting phase makes a more significant contribution to the stray current, and the rear wheel leakage during the braking phase makes a more substantial contribution to the stray current.

(2) Rail corrosion is a dynamic corrosion process, and the rail corrosion in the insulation damaged area is more severe than that without insulation. In contrast, the rail corrosion near the substation is just the opposite.

(3) The corrosion of the buried pipeline is closely related to the damaged insulation area. The corrosion of pipelines in areas without damaged insulation is more severe than in some damaged insulation areas. Therefore, buried pipelines' corrosion degree and corrosion area can be reasonably evaluated by effectively detecting damaged insulation areas to guide targeted excavation and maintenance.

Data Availability

The data (experimental results) used to support the findings of this study are included in the article.

Conflicts of Interest

The authors declare that there are no conflicts of interest regarding the publication of this paper.

Acknowledgments

This work was supported in part by the Natural Science Foundation of China under grant 51807065 and in part by the Key Research and Development Plan of Jiangxi Province under grant 20202BBEL53015.

References

[1] S. A. Memon and P. Fromme, "Stray Current Corrosion and Mitigation: a synopsis of the technical methods used in dc transit systems," *IEEE Electrification Magazine*, vol. 2, no. 3, pp. 22–31, 2014.

[2] S. W. Chen, M. Y. Qin, D. X. Liu, and J. H. Gong, "Study on erosion risk prediction of wet gas gathering and transmission pipeline in high sulfur gas field," *Natural gas and oil*, vol. 33, no. 1, pp. 80–83+12, 2015.

[3] Z. F. Zhao, *Study on Dynamic Evaluation Method of Safety for Corrosion protection System of Long-Distance Pipeline*, Xi'an University of Science and Technology, Xi'an, China, 2017.

[4] A. L. Cao, *Study on Stray Current Corrosion protection of Buried Metal Pipelines*, Chongqing University, Chongqing, China, 2010.

[5] M. Niasati and A. Gholami, "Overview of stray current control in DC railway systems," in *Proceedings of the International Conference on Railway Engineering-Challenges for Railway Transportation in Information Age*, pp. 1–6, Hong Kong, China, March 2008.

[6] Y. T. Zhang, "Traction power supply technology for the fourth return track of urban rail transit," *Modern urban transit*, vol. 4, pp. 8–10+125, 2011.

[7] C. Goodman, J. Allan, J. Jin, and K. Payne, "Single pole-to-earth fault detection and location on a fourth-rail DC railway system," *IEE Proceedings - Electric Power Applications*, vol. 151, no. 4, pp. 498–504, 2004.

[8] D. F. Yan, N. Y. Liu, P. B. Yuan, J. Shu, and Y. E. Li, "Corrosion of buried steel pipelines by stray current in Metro maintenance base and protective measures," *Corrosion & Protection*, vol. 34, no. 8, pp. 739–742, 2013.

[9] D. Paul, "DC stray current in rail transit systems and cathodic protection [history]," *IEEE Industry Applications Magazine*, vol. 22, no. 1, pp. 8–13, 2016.

[10] I. Cotton, C. Charalambous, P. Aylott, and P. Ernst, "Stray current control in DC mass transit systems," *IEEE Transactions on Vehicular Technology*, vol. 54, no. 2, pp. 722–730, 2005.

[11] Z. M. Zhang, *Study on protection Measures against Stray Current in Metro*, Southwest Jiaotong University, Chengdu, China, 2015.
[12] N. M. J. Dekker, "Stray current control-an overview of options [DC traction systems]," *IEE Seminar on DC Traction Stray Current Control - Offer a Stray a Good Ohm?* pp. 8-810, 1999.
[13] J. Zhu and C. Q. Zhu, "Study on the distribution of stray current and rail potential in multi-section of urban rail transit," *China Science and Technology Information*, vol. 11, pp. 90-91, 2020.
[14] K. Yu, *Study on Simulation of Metro Stray Current Based on DEGS*, Southwest Jiaotong University, Chengdu, China, 2014.
[15] X. H. Han, W. Liu, and S. F. Jie, "Calculation of cross-sectional area of metro stray current collection network," *Urban Mass Transit*, vol. 18, no. 10, pp. 98–101+105, 2015.
[16] L. Huang, G. F. Du, J. Wang, and J. Tian, "Simulation study on dynamic drainage and rail potential control of urban rail reflux system," *Railway Standard Design*, vol. 63, no. 10, pp. 152–158, 2019.
[17] G. Du, J. Wang, X. Jiang, D. Zhang, L. Yang, and Y. Hu, "Evaluation of rail potential and stray current with dynamic traction networks in multitrain subway systems," *IEEE Transactions on Transportation Electrification*, vol. 6, no. 2, pp. 784–796, 2020.
[18] J. Gu, X. Yang, T. Q. Zheng, Z. Shang, Z. Zhao, and W. Guo, "Negative resistance converter traction power system for reducing rail potential and stray current in the urban rail transit," *IEEE Transactions on Transportation Electrification*, vol. 7, no. 1, pp. 225–239, 2021.
[19] G. F. Du, C. L. Wang, J. H. Liu, G. X. Li, and D. L. Zhang, "Effect of over zone feeding on rail potential and stray current in DC mass transit system," *Mathematical Problems in Engineering*, vol. 2016, Article ID 6304726, 2016.
[20] H. Z. Li, "Calculation of rail potential and stray current based on centralized parameter model of reflux system," *Modern urban transit*, vol. 6, pp. 20–23, 2020.
[21] T. T. Ke, J. M. Fang, Y. H. Qian, and Z. B. Peng, "Effects of metro stray current on cathode protection of buried metal pipelines," *Urban Mass Transit*, vol. 20, no. 3, pp. 90–93, 2017.
[22] K. Zakowski, K. Darowicki, A. Jazdzewska, S. Krakowiak, M. Gruszka, and J. Banas, "Electrolytic corrosion of water pipeline system in the remote distance from stray currents-Case study," *Case Studies in Construction Materials*, vol. 4, pp. 116–124, 2016.
[23] X. Hao and D. L. Li, "New risk to buried steel pipe anti-corrosion system caused by DC stray current of rail transit," *Urban Georgia*, vol. 3, pp. 12–17, 2016.
[24] Z. C. Cai, X. W. Zhang, and J. Zhang, "Research on theoretically modelling and quantitatively calculating stray current corrosion in a subway system," *International Journal of Electrochemical Science*, vol. 2020, no. 15, pp. 6626–6644, 2020.
[25] H. R. Wang, *Design of Stray Current Monitoring System for Urban Rail Transit*, Southwest Jiaotong University, Chengdu, China, 2007.
[26] S. R. Allahkaram, M. Isakhani-Zakaria, M. Derakhshani, M. Samadian, H. Sharifi-Rasaey, and A. Razmjoo, "Investigation on corrosion rate and a novel corrosion criterion for gas pipelines affected by dynamic stray current," *Journal of Natural Gas Science and Engineering*, vol. 26, pp. 453–460, 2016.
[27] A. O. S. Solgaard, M. Carsana, M. R. Geiker, A. Küter, and L. Bertolini, "Experimental observations of stray current effects on steel fibres embedded in mortar," *Corrosion Science*, vol. 74, pp. 1–12, 2013.
[28] Y.-S. Tzeng and C.-H. Lee, "Analysis of rail potential and stray currents in a direct-current transit system," *IEEE Transactions on Power Delivery*, vol. 25, no. 3, pp. 1516–1525, 2010.
[29] Z. Chen, D. Koleva, and K. van Breugel, "A review on stray current-induced steel corrosion in infrastructure," *Corrosion Reviews*, vol. 35, no. 6, pp. 397–423, 2017.
[30] L. Bertolini, M. Carsana, and P. Pedeferri, "Corrosion behaviour of steel in concrete in the presence of stray current," *Corrosion Science*, vol. 49, no. 3, pp. 1056–1068, 2007.
[31] J. G. Yu, "The effects of earthing strategies on rail potential and stray currents in DC transit railways," in *Proceedings of the 1998 International Conference on Developments in Mass Transit Systems Conf. Publ. No. 453)*, pp. 303–309, London, UK, April 1998.
[32] L. Cai, J. G. Wang, and Y. D. Fan, "Influence of the track-to-earth resistance of subway on stray current distribution," *High Voltage Engineering*, vol. 41, no. 11, pp. 3604–3610, 2015.
[33] J. P. Xu, "Analysis of urban rail transit stray current in buried pipeline and protective measures," *Urban Mass Transit*, vol. 20, no. 7, pp. 60–64, 2017.
[34] X. F. Yang, H. K. Wang, and Q. L. Zheng, "Influence of finite boundary fringe effect on the rail potential in DC traction power supply system," *Journal of Beijing Jiaotong University*, vol. 44, no. 3, pp. 1–11, 2020.